Université de Mons
Faculté Polytechnique – Service de Mécanique Rationnelle, Dynamique et Vibrations
31, Bld Dolez - B-7000 MONS (Belgique)
065/37 42 15 – georges.kouroussis@umons.ac.be

G. Kouroussis, X. Siebert, B. Olivier, A coupled lumped mass system for soil representation in railway dynamics and vibration modelling, *In XXVI^e Congrès Français de Mécanique*, Metz (France), August 25–29, 2005. Association Française de Mécanique

A Coupled Lumped Mass System for Soil Representation in Railway Dynamics and Vibration Modelling

G. KOUROUSSIS[a], X. SIEBERT[b], B. OLIVIER[c]

a. Université de Mons – UMONS, Faculty of Engineering, Department of Theoretical Mechanics, Dynamics and Vibrations, Place du Parc, 20 — 7000 Mons (BELGIQUE), georges.kouroussis@umons.ac.be

b. Université de Mons – UMONS, Faculty of Engineering, Department of Mathematics and Operational Research, Place du Parc, 20 — 7000 Mons (BELGIQUE), xavier.siebert@umons.ac.be

c. Université de Mons – UMONS, Faculty of Engineering, Department of Theoretical Mechanics, Dynamics and Vibrations, Place du Parc, 20 — 7000 Mons (BELGIQUE), bryan.olivier@umons.ac.be

Résumé :

L'interaction entre le véhicule et la voie joue un rôle capital dans la dynamique des véhicules ferroviaires, ainsi que dans l'analyse vibratoire des véhicules et de la voie elle-même. Le contact roue-rail est fortement influencé par la flexibilité de la voie. Si cette flexibilité est généralement intégrée dans les simulations dynamiques actuelles, il n'en va pas de même pour celle du sol, souvent considéré comme rigide. Cette simplification s'explique principalement par la complexité et la charge de calcul élevée des modèles de sol par rapport à ceux des véhicules et de la voie. Ce travail propose une solution élégante et innovante : un modèle condensé du sol, limité à la zone ferroviaire. Ce modèle repose sur une série de masses ponctuelles interconnectées par des ressorts et des amortisseurs, jouant ainsi le rôle de fondation. Ce modèle de fondation, baptisé CLM (pour Coupled Lumped Mass), s'inspire du modèle analogue de Lysmer. La configuration masses-ressorts-amortisseurs introduite ici présente cinq paramètres indépendants de la fréquence, permettant de modéliser l'interaction entre les fondations et la surface de contact entre la voie et le sol. Ce couplage voie-sol s'exprime généralement dans une gamme de fréquences inférieure à 100 Hz. Des expressions analytiques ont été établies pour calibrer ce modèle dans le cas de sols homogènes ou stratifiés en couches horizontales. Initialement réalisée manuellement, cette calibration s'appuie désormais sur une technique de réseaux de neurones, qui établit des relations analytiques directes entre les propriétés élastiques du sol (module de Young, coefficient de Poisson, masse volumique, amortissement structurel) et les paramètres du modèle CLM (masse, raideurs, coefficients d'amortissement). Des exemples numériques illustrent l'application du modèle, en mettant en évidence l'influence de la rigidité et de l'amortissement du sol. L'analyse vibratoire d'une voie sur différentes fondations révèle que le modèle CLM reproduit avec précision l'interaction dynamique entre la voie et le sol. Ce modèle s'avère donc fiable pour des simulations dynamiques complètes intégrant le véhicule, la voie et la fondation.

Abstract :

The interaction between the vehicle and the track plays a crucial role in the dynamics of railway vehicles, as well as in the vibration analysis of vehicle and track. The wheel-rail contact is strongly influenced by the flexibility of the track. While this flexibility is commonly included in current dynamic simulations, the same cannot be said for the soil, which is often assumed to be rigid. This simplification is primarily due to the complexity and high computational cost of soil models compared to vehicle-track models. This study proposes an elegant and innovative solution : a condensed soil model focused exclusively on the railway area. This model is based on a series of lumped masses interconnected by spring and dashpot elements, effectively representing the foundation. This foundation model, named CLM (Coupled Lumped Mass), is inspired by the Lysmer analogue model. The proposed mass–spring–damper configuration features five frequency–independent parameters, enabling the modelling of interactions between the foundation and the contact surface between the track and the soil. This track-soil coupling generally occurs within a frequency range below 100 Hz. Analytical expressions have been derived to tune this model for homogeneous or horizontally stratified soils. Initially performed manually, this updating is now assisted by an artificial neural networks technique, which establishes direct analytical relationships between the soil's elastic properties (Young's modulus, Poisson's ratio, density, structural damping) and the parameters of the CLM model (mass, stiffness, damping coefficients). Numerical examples illustrate the application of the model, highlighting the influence of soil rigidity and damping. The vibration analysis of a track on different foundation models demonstrates that the CLM model accurately reproduces the dynamic interaction between the track and the soil. This model thus proves to be reliable for comprehensive dynamic simulations that integrate the vehicle, track and foundation.

Mots clefs : ferroviaire, méthode des éléments finis, modèle CLM, réseaux de neurones

Keywords : railway, finite element model, CLM model, neural networks

1 Introduction

Dynamic simulation has become essential in the railway sector, whether for studying the dynamic and vibratory behaviour of vehicles or for designing anti-vibration solutions to be mounted on the railway network [1, 2]. In the first case, the multibody approach makes it possible to account for large displacements as well as the vehicle's non-linear behaviour. The second case, often associated with a finite element or discrete element approach, generally relies on a modal analysis of the problem, where the study is conducted by comparing transfer functions. In all cases, these models, often referred to as digital twins, provide a credible alternative to experimental approaches [3].

In recent years, these models have been refined to adopt a more global approach : the track is now often integrated into vehicle dynamic simulations, allowing for the consideration of the wheel/rail interaction and the resulting dynamic coupling. Different coupling strategies can thus

be employed, such as co-simulation between a multibody model and a finite element model [4], or an approach in the frequency domain [5]. Ignoring coupling involves certain simplifying assumptions, thereby limiting the applicability of the model. Additionally, ground effects must also be considered, as they have a significant influence up to frequencies of 100 Hz [6].

Unfortunately, the inclusion of the track complicates modeling. While the frequency domain benefits from mathematical tools that facilitate this coupling, the time-domain approach (numerical integration of the equations of motion) is hindered by relatively long computation times, beyond the coupling itself. In this regard, vehicle/track/ground co-simulation studies provide a good illustration of this issue (e.g., [7, 8]).

The study of track/soil coupling and the associated degree of dynamic interaction is not new. The analytical work of Sarfield et al. [9] and Rücker [10] initially focused on the potential interaction between sleepers and the ground of a railway track in the absence of intermediate elements such as ballast. Later, Knothe and Wu [6] demonstrated that track receptances are better predicted at low frequencies when the soil is modeled as a half-space rather than using the Winkler foundation, the latter being represented by spring elements distributed along the rail, which is itself modeled as a continuously supported beam in bending. To fully capture this coupling effect, two mechanisms must be considered (Figure 1) :

1. the transfer of vibrations between sleepers through the rail (top coupling, generally included in track models) and
2. the transfer of vibrations through the soil (bottom coupling).

In the Winkler formulation, the flexibility of the soil beneath the sleepers (direct coupling) is accounted for, but not the bottom coupling (indirect coupling).

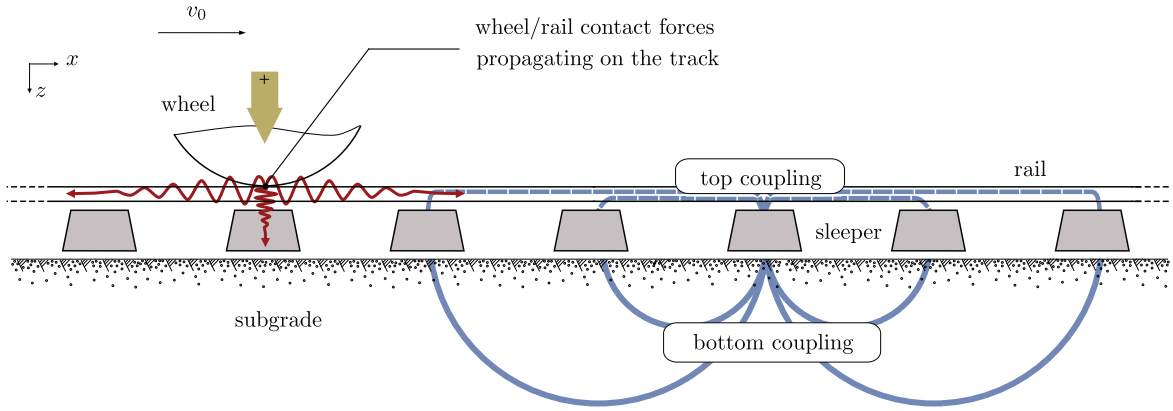

FIGURE 1 – Two modes of vibration transfer between sleepers [11]

To avoid complex and computationally expensive models, this paper proposes focusing on discrete models, such as those used in various predictive approaches for vibrations induced by railway traffic, and leveraging machine learning techniques to optimize the parameter definition process. An existing model, called the CLM model [11, 12], is used with a new approach to characterize the parameters that define it, relying on machine learning to adjust these parameters based on the dynamic characteristics commonly used in geotechnics.

2 Railway modelling

It is commonly accepted that the multibody system approach is the preferred tool for studying the vibrational behaviour of a railway vehicle, taking into account large motions (inducing non-linear behaviours), complex suspension models, or even loss of contact between solids (such as the wheel–rail contact). All of this is, of course, possible through numerical integration in the time domain of the dynamic motion equations obtained by the method. Track models are less numerous, focusing on a specific element (e.g., rail deflection/deformation, ballast characterization). Early track modelling approaches, based on the assumption that the rail could be represented as a single beam (typically of the Euler–Bernoulli type) resting on a Winkler foundation, were abandoned in favour of multilayer models, with each layer characterizing a specific track component (rail pad, sleeper, ballast, ...). Single-layer methods were useful for studying the very low-frequency characteristics of the track. Two-layer models were also proposed and were considered an improvement over single-layer models, as they allowed for the simulation of rail pads, sleepers, and ballast. It should also be noted that track support conditions (subgrade) have a significant effect on track stiffness and therefore influence its dynamic response. In the previously mentioned models, the track base was assumed to be rigid. While this assumption may be suitable for tracks where the subgrade has a stiffness comparable to that of the track, discrepancies arise when the supporting material is softer [13]. Consequently, research has also been conducted to model the subgrade as an elastic half–space. Beyond the chosen model, the difficulty lies in estimating the values of the track parameters, for which the physical meaning is not always clear (e.g., modelling a material with a behaviour as complex as ballast using a simple spring-damper system).

The model proposed here is a two–layer 2D model [14,15], considering only the inertial effects of the track and sleepers, as illustrated in Figure 2. The flexible rail is characterized by its Young's modulus E_r, geometric moment of inertia I_r, cross-sectional area A_r, and mass density ρ_r. The viscoelastic properties of the rail pads and ballast are modelled using springs and dampers, with stiffness and damping parameters (k_p and d_p for the rail pads, k_b and d_b for the ballast). The subgrade model is also a discrete model, described later, by first analysing the dynamic behaviour of the subgrade as a foundation [16].

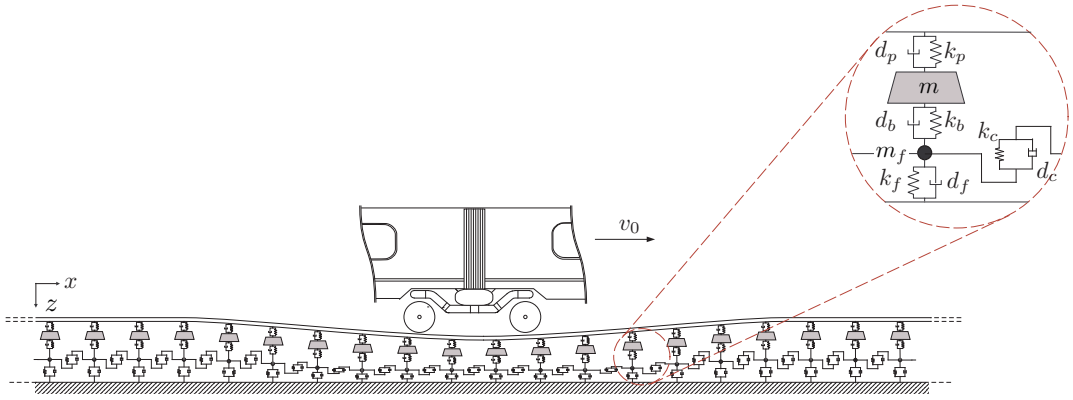

FIGURE 2 – The flexible 2D track, considering a condensed soil (represented by the CLM model)

3 From a finite element to a discrete model

3.1 The Lysmer analogue model

The dynamic response of a vertically loaded massive foundation (aka subgrade) can be modelled using a single-degree-of-freedom mass–spring–dashpot oscillator, where the stiffness and damping coefficients vary with frequency. Lysmer advanced this approach by proposing the use of frequency-independent parameters, simplifying the representation of the system (Figure 3).

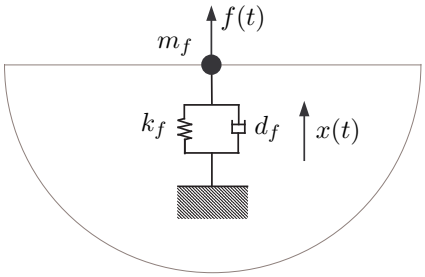

FIGURE 3 – Lysmer analogue modelling of foundation

This approximation gained immediate success, Lysmer's so-called "analogue" model can replicates the soil impedance as functions of the circular frequency ω :

$$P(\omega) = k_f - \omega^2 m_f + j\omega d_f \tag{1}$$

Here, the real part of the impedance varies with frequency, consistent with observed physical behaviour. It is important to note that the parameter m_f is not directly related to the actual foundation mass since a massless foundation can be assumed. Figure 4 illustrates the comparison of the real parts (parabolic-shaped curve) and imaginary parts (linear evolution) of the impedance between this discrete approach and a finite element modelling after fitting the frequency-independent parameters k_f, d_f and m_f. The results confirm that the Lysmer analogue model accurately replicates the actual response. However, this approach remains simplistic when considering multiple interconnected foundations.

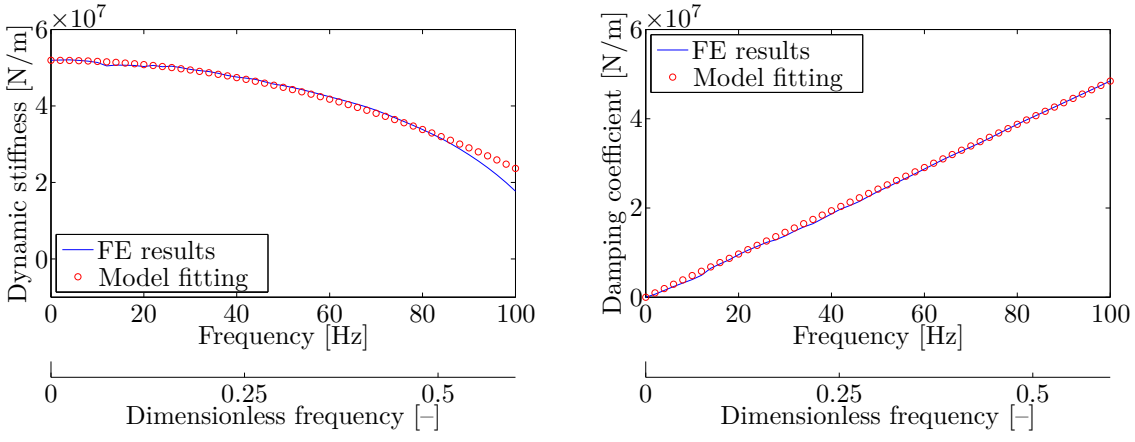

(a) Real part (b) Imaginary part

FIGURE 4 – Exemple of fitting vertical impedance with numerical model

3.2 CLM model

The proposed model, depicted schematically in Figure 5, overcomes the limitation mentioned above and is composed of discrete masses, springs, and dampers. The CLM model for the foundation (i.e., the sleeper-through-the-ballast contact area) extends Lysmer analogue foundation by incorporating additional coupling elements. Alongside the foundation's mass (m_f), stiffness (k_f), and damping (d_f), extra spring–dashpot systems with stiffness (k_c) and damping (d_c) are included to simulate the interaction between sleeper-foundation contact areas (adjacent foundations). Simplified transmissibility expressions have been derived to determine these five parameters for different soil conditions, whether homogeneous or layered. Notably, the damping parameter d_c may assume negative values to account for the propagation delay of ground waves [12].

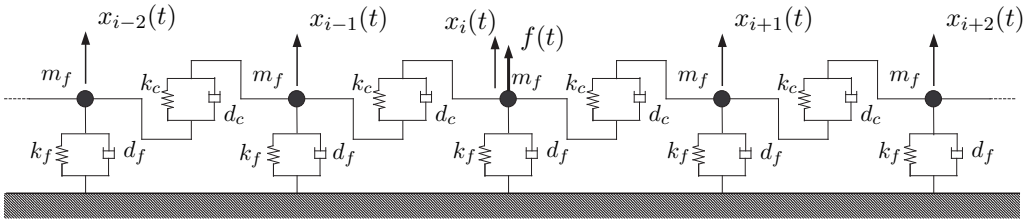

FIGURE 5 – The CLM model : a multi-foundation model for soil–foundation and foundation–to–foundation interaction [12]

When a force is applied to the i-th mass, the overall impedances P_1 and P_2 corresponding to each vertical displacement x_j are given by [12] :

$$P_1(\omega) = \frac{F(\omega)}{\sum_{j=-n}^{n} X_j(\omega)} = k_f - \omega^2 m_f + \mathrm{j}\omega d_f \tag{2}$$

$$P_2(\omega) = \frac{F(\omega)}{\sum_{j=-n}^{n} (-1)^j X_j(\omega)} = (k_f + 4k_c) - \omega^2 m_f + \mathrm{j}\omega(d_f + 4d_c) \tag{3}$$

where $F(\omega)$ and $X_j(\omega)$ represent the Fourier transforms of the applied force $f(t)$ and displacements $x_j(t)$, respectively. These equations provide distinct close relationships for calibrating the CLM model parameters. The values of these parameters can be efficiently determined using a finite element model of the soil by applying a known force at a specific mass and recording the vertical displacement spectrum at n points, ensuring sufficient spatial coverage to capture the full ground wave propagation.

3.3 Calibrating using a soil finite element model

For each considered soil type, a finite element numerical simulation is conducted, for example, using ABAQUS (Figure 6). To mitigate spurious wave reflections, specific boundary conditions are applied through infinite elements. The dynamic simulation provides vertical displacement data at n points on the soil surface when a vertical force $f(t)$ is applied at the surface. These displacement histories are then combined with Eqs. (2) and (3) to manually calibrate the CLM model parameters corresponding to the given soil type.

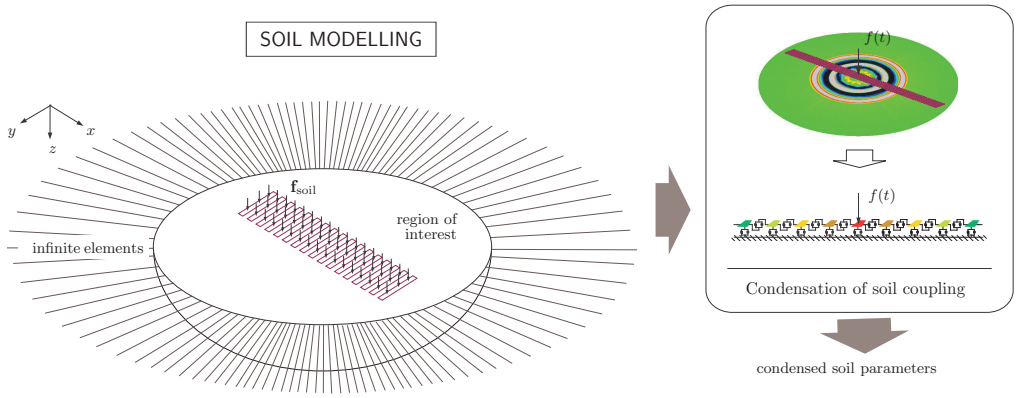

FIGURE 6 – The finite element model for the soil, used to calibrate the CLM model

This calibration process is labour–intensive, as it necessitates running a separate numerical simulation for each specific soil configuration. These simulations are computationally expensive, often requiring several hours due to the large number of finite elements involved. Additionally, the calibration involves manual adjustments, where the parameters P_1 and P_2 are iteratively refined to minimize local discrepancies in the real and imaginary spectra between the CLM model and the ABAQUS simulation.

3.4 On the use of neural networks

Artificial neural networks are widely used machine learning techniques that provide new insights into fitting operations compared to traditional methods such as numerical optimization or statistical approaches [17]. Training a neural network to approximate the relationship between inputs and outputs is particularly effective for complex and/or non-linear problems. For this study, the structure of the artificial neural networks designed to estimate the parameters of the CLM model is defined as follows :

— **Number of Networks :** Five independent neural networks are implemented, each dedicated to predicting one specific CLM model parameter (m_f, k_f, d_f, k_c, or d_c).

— **Input Layer :** Each network receives normalized soil characteristics as input, including Young's modulus (E), density (ρ), Poisson's ratio (ν), and the viscous damping coefficient (β). These inputs are typically represented by four neurons. To enhance network convergence during training, the inputs to the neural networks are normalized within the range of 0 to 1. Although this normalization is not strictly required, it helps maintain synaptic weight values within a consistent order of magnitude. The input values for the neural networks are obtained by normalizing the soil characteristics using a predefined standard value : $E_{nom} = 400\,\text{MPa}$, $\rho_{nom} = 2600\,\text{kg/m}^3$, $\nu_{nom} = 0.45$, $\beta_{nom} = 0.0013\,\text{s}$.

— **Output Layer :** Each network has a single output neuron that provides the corresponding normalized CLM model parameter (m_f, k_f, d_f, k_c, or d_c). The expected maximum values retained for the CLM model parameters are : $k_f = 120\,\text{MN/m}$, $d_f = 350\,\text{kNs/m}$, $m_f = 260\,\text{kg}$, $k_c = 60\,\text{MN/m}$, $d_c = -50\,\text{kNs/m}$. It is important to note that the cross-damping coefficient d_c remains negative to take into account for the effects of wave delay and material damping.

— **Hidden Layers :** The architecture of hidden layers varies based on the complexity re-

quired. Each network generally consists of a single hidden layer containing between 10 and 20 neurons, utilizing activation functions such as the sigmoid function. The matrix representation of this function is

$$\text{sigm}\left(\begin{bmatrix} & \vdots & \\ \cdots & a_{ij} & \cdots \\ & \vdots & \end{bmatrix}\right) = \begin{bmatrix} & \vdots & \\ \cdots & \frac{1}{1+e^{-a_{ij}}} & \cdots \\ & \vdots & \end{bmatrix} . \tag{4}$$

— **Training :** The networks are trained using back propagation with an appropriate optimizer and a loss function, such as mean squared error, to minimize prediction errors. Training data is generated from numerical simulation results, ensuring sufficient variability in soil properties for better generalization.

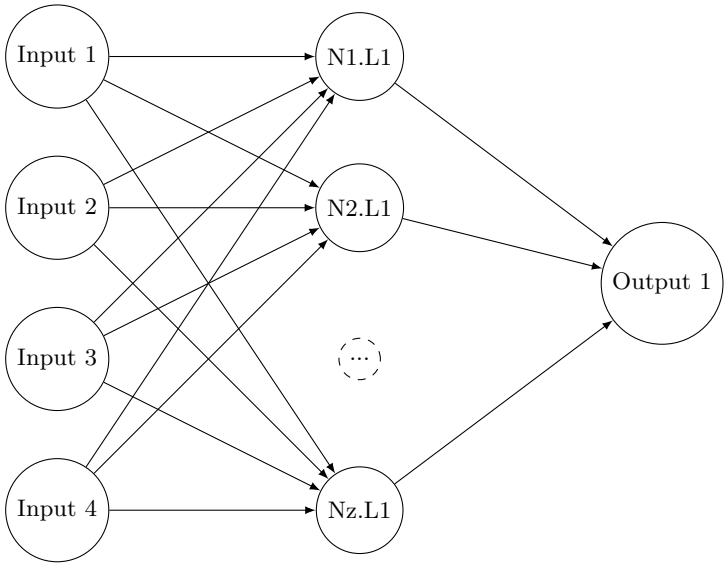

FIGURE 7 – Structure of the five artificial neural networks to calculate the parameters of the CLM model

Once the neural networks have been trained, they can be used to predict the CLM model parameters for a given soil. This is achieved using the following matrix relations :

$$m_f = 260\ \text{sigm}\left(\text{sigm}\left(\left[\tfrac{E}{400} \quad \tfrac{\rho}{2600} \quad \tfrac{\nu}{0.45} \quad \tfrac{\beta}{0.0013}\right].\mathbf{W}_{1mf}\right).\mathbf{W}_{2mf}\right) , \tag{5}$$

$$k_f = 120\ \text{sigm}\left(\text{sigm}\left(\left[\tfrac{E}{400} \quad \tfrac{\rho}{2600} \quad \tfrac{\nu}{0.45} \quad \tfrac{\beta}{0.0013}\right].\mathbf{W}_{1kf}\right).\mathbf{W}_{2kf}\right) , \tag{6}$$

$$d_f = 350\ \text{sigm}\left(\text{sigm}\left(\left[\tfrac{E}{400} \quad \tfrac{\rho}{2600} \quad \tfrac{\nu}{0.45} \quad \tfrac{\beta}{0.0013}\right].\mathbf{W}_{1df}\right).\mathbf{W}_{2df}\right) , \tag{7}$$

$$k_c = 60\ \text{sigm}\left(\text{sigm}\left(\left[\tfrac{E}{400} \quad \tfrac{\rho}{2600} \quad \tfrac{\nu}{0.45} \quad \tfrac{\beta}{0.0013}\right].\mathbf{W}_{1kc}\right).\mathbf{W}_{2kc}\right) , \tag{8}$$

$$d_c = -50\ \text{sigm}\left(\text{sigm}\left(\left[\tfrac{E}{400} \quad \tfrac{\rho}{2600} \quad \tfrac{\nu}{0.45} \quad \tfrac{\beta}{0.0013}\right].\mathbf{W}_{1dc}\right).\mathbf{W}_{2dc}\right) . \tag{9}$$

Input and output data are normalized to facilitate training and improve convergence. After training, the output values are denormalized to obtain the actual CLM model parameters.The weight matrices $\mathbf{W}_1$ and $\mathbf{W}_2$, obtained after complete training and validation, are presented in Figure 8.

$$
\mathbf{W}_{1kf} = \begin{bmatrix}
0.2337 & 0.3423 & 0.1602 & 0.2900 & 0.2538 & 0.2356 & -3.0213 & 0.3498 & 0.3771 & -12.8553 & -3.2296 & 0.2913 & 0.2802 & -4.6937 & 4.8994 & 0.4376 & -2.3406 & -4.4330 & 0.3672 & 5.7519 \\
-1.9139 & -1.0948 & -1.9523 & -0.4483 & -0.2939 & -0.4717 & -0.6484 & -0.7898 & -1.3874 & 1.1450 & -0.5458 & -1.8384 & -0.4022 & 0.5523 & -4.1841 & -1.6970 & -1.1497 & -0.1869 & -1.7358 & -2.4261 \\
-1.2335 & -1.8107 & -1.1651 & -1.9641 & -1.9609 & -1.8965 & -1.4299 & -1.9260 & -1.7281 & 0.6165 & -1.3661 & -1.3574 & -1.9651 & -0.7494 & -8.2312 & -1.6083 & -1.6188 & -0.8915 & -1.5150 & -2.8182 \\
0.5614 & -0.2235 & 0.5931 & -0.0388 & -0.0561 & -0.0957 & -0.1825 & -0.0822 & -0.2609 & -0.0921 & -0.1964 & 0.2602 & -0.0412 & 0.5215 & 0.1303 & -0.0181 & -0.1380 & -0.1712 & 0.0117 & -0.0032
\end{bmatrix}
$$

$$
\mathbf{W}_{1df} = \begin{bmatrix}
-1.1599 & -0.5239 & 0.3472 & -1.7549 & 4.3717 & 0.7200 & 0.1572 & -1.1669 & -21.3523 & -5.8452 & -0.6298 & -1.6406 & -4.4335 & 10.2036 & -1.3802 & -1.7975 \\
-0.7688 & -0.6883 & -0.4747 & -3.3744 & -1.1808 & -0.3466 & -0.5340 & -0.7602 & -2.3608 & -0.9177 & -0.7039 & -0.8235 & -0.7240 & -6.9995 & -0.7959 & -0.8399 \\
-0.9336 & -1.4809 & -2.3192 & 0.5022 & -4.7797 & -2.7029 & -2.1276 & -0.9330 & 5.4400 & -2.7163 & -1.3852 & -0.5626 & -2.4359 & -7.6155 & -0.7564 & -0.4568 \\
0.2836 & -0.0190 & -0.2564 & -1.5101 & 2.1968 & -0.3045 & -0.2248 & 0.3153 & -5.4261 & 11.2837 & 0.0311 & 0.5243 & 9.8255 & -0.3646 & 0.3868 & 0.6046
\end{bmatrix}
$$

$$
\mathbf{W}_{1kc} = \begin{bmatrix}
-0.8516 & -0.8503 & 3.2659 & -0.8357 & -0.8503 & -0.8508 & -19.6738 & -0.4493 & -0.8333 & -0.8450 \\
-0.6032 & -0.6070 & 0.2534 & -0.6480 & -0.6072 & -0.6055 & 1.5493 & -4.0142 & -0.6553 & -0.6222 \\
-0.1191 & -0.1174 & -2.5374 & -0.1006 & -0.1174 & -0.1181 & 0.6980 & 4.1316 & -0.0975 & -0.1112 \\
-0.0320 & -0.0326 & 0.0278 & -0.0390 & -0.0326 & -0.0324 & 0.4889 & -0.0762 & -0.0401 & -0.0349
\end{bmatrix}
$$

$$
\mathbf{W}_{1mf} = \begin{bmatrix}
-0.0383 & -0.3422 & -0.3422 & -6.8758 & -0.3422 & -0.3422 & -0.7192 & 0.6398 & -18.7953 & -0.3422 \\
-4.8286 & -1.9677 & -1.9676 & -8.0574 & -1.9676 & -1.9676 & 2.9375 & -3.0118 & 1.2588 & -1.9676 \\
-0.9171 & -0.9369 & -0.9370 & -15.2688 & -0.9370 & -0.9369 & -0.6858 & 0.0309 & -3.2220 & -0.9370 \\
-13.0434 & -1.9213 & -1.9213 & 25.9524 & -1.9213 & -1.9213 & -1.6652 & -1.8106 & 0.9288 & -1.9213
\end{bmatrix}
$$

$$
\mathbf{W}_{1dc} = \begin{bmatrix}
-3.7770 & -0.9336 & 2.0538 & -0.8659 & -1.1368 & -4.9684 & -6.4280 & -1.5592 & -7.8356 & 1.9337 & 0.8577 & -0.3505 & -1.6817 & -1.2849 \\
0.9488 & -0.6480 & -1.3385 & -1.0742 & 0.1718 & 1.0041 & 0.2924 & -1.8640 & 4.7434 & 0.5528 & -4.4857 & 1.5108 & -0.1700 & -2.6191 \\
1.2461 & -0.3956 & -1.2443 & -1.0379 & 0.9733 & 1.6908 & -0.1406 & -1.9841 & 3.1849 & -0.7652 & 0.7584 & -1.8860 & -0.4967 & -1.9863 \\
5.7794 & -2.1228 & 2.2962 & 1.9532 & -2.0806 & -1.6053 & 0.2739 & 0.4248 & -6.8101 & 4.5515 & 1.6710 & 3.0052 & -1.8178 & 0.8520
\end{bmatrix}
$$

$$
\mathbf{W}_{2kf} = \begin{bmatrix}
-1.6385 \\ -1.5323 \\ -1.6331 \\ -1.4418 \\ -1.4247 \\ -1.4369 \\ 2.4665 \\ -1.4906 \\ -1.5851 \\ -5.9541 \\ 2.5873 \\ -1.6175 \\ -1.4364 \\ 2.5224 \\ 3.7912 \\ -1.6397 \\ 1.5088 \\ 3.3496 \\ -1.6206 \\ 4.6321
\end{bmatrix}
\quad
\mathbf{W}_{2df} = \begin{bmatrix}
-1.5142 \\ -1.4748 \\ -1.4355 \\ 4.3698 \\ 3.1720 \\ -1.2496 \\ -1.4594 \\ -1.3280 \\ -2.3226 \\ -2.7940 \\ -1.4343 \\ -1.6698 \\ 3.8536 \\ -1.0587 \\ -1.6311 \\ -1.6785
\end{bmatrix}
$$

$$
\mathbf{W}_{2kc} = \begin{bmatrix}
-1.4535 \\ -1.4534 \\ 2.3170 \\ -1.4527 \\ -1.4534 \\ -1.4535 \\ -1.9760 \\ 1.7620 \\ -1.4526 \\ -1.4532
\end{bmatrix}
\quad
\mathbf{W}_{2mf} = \begin{bmatrix}
44.1789 \\ -3.2990 \\ -3.2991 \\ -0.5109 \\ -3.2991 \\ -3.2991 \\ 2.6954 \\ -2.1951 \\ -2.5960 \\ -3.2991
\end{bmatrix}
\quad
\mathbf{W}_{2dc} = \begin{bmatrix}
-1.8316 \\ -1.3537 \\ -1.9485 \\ -1.9925 \\ 0.7837 \\ 3.1790 \\ -4.5897 \\ 1.6189 \\ -1.9946 \\ 3.5398 \\ -2.1154 \\ -1.9860 \\ -1.6500 \\ 5.7333
\end{bmatrix}
$$

FIGURE 8 – Weight matrices of the trained neural networks

3.5 Sensitivity analysis

At this stage, a sensitivity analysis can be conducted to visualize the influence of the soil input parameters on the parameters of the CLM model. Without going into a detailed analysis, Figure 9 illustrates the sensitivity of each parameter and highlights their influence on the model's elastic properties (k_i *vs.* E and ν), dissipative properties (d_i *vs.* E and β), and inertial properties (m_f *vs.* E and ρ). It turns out that Poisson's ratio has little influence on all parameters and that only the foundation mass is weakly dependent on Young's modulus.

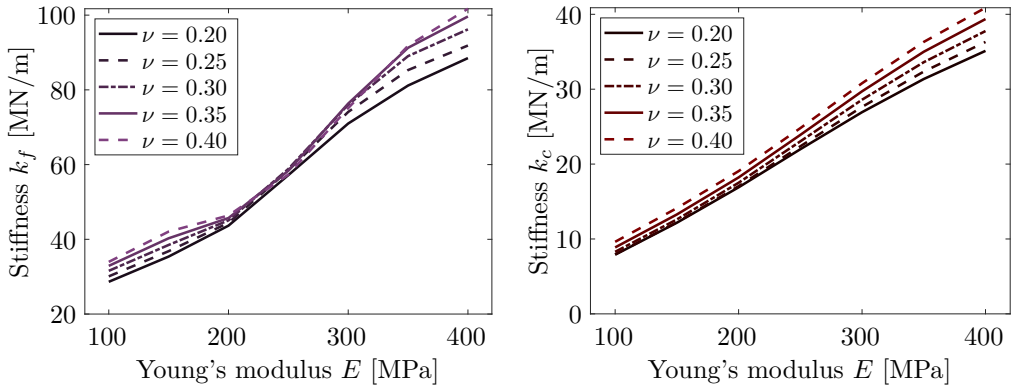

(a) On the stiffness k_f

(b) On the stiffness k_c

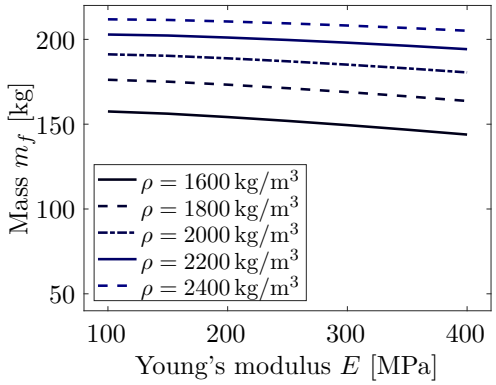

(c) On the mass m_f

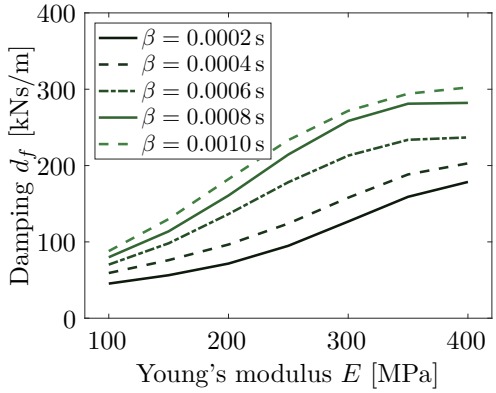

(d) On the damping d_f

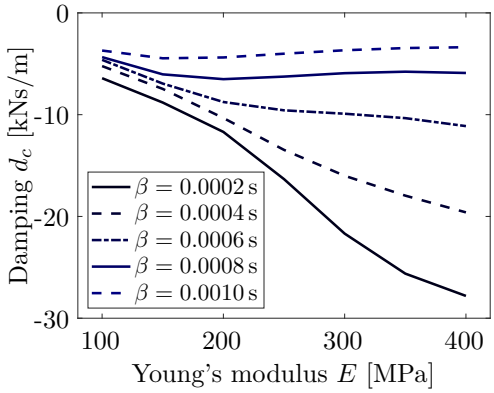

(e) On the damping d_c

FIGURE 9 – An overall sensitivity analysis of the soil parameters on the CLM model parameters

4 Results

Table 1 presents a sample of the soil parameters values, comparing them with manually obtained data. This comparison demonstrates the effectiveness of the implemented neural network, with an accuracy that is entirely acceptable. The results correspond to a homogeneous soil characterized by the following properties : Young's modulus $E = 160\,\text{MPa}$, density $\rho = 1600\,\text{kg/m}^3$, Poisson's ratio $\nu = 0.30$ and viscous damping coefficient $\beta = 0.0004\,\text{s}$.

TABLE 1 – Example of Comparative Results on the CLM Model

	m_f [kg]	k_f [MN/m]	d_f [kNs/m]	k_c [MN/m]	d_c [kNs/m]
Parameters manually calibrated	146.78	36.24	73.56	12.43	−8.25
Parameters obtained using Eqs. (6)–(9)	150.54	38.35	77.77	13.91	−8.62

To demonstrate the beneficial effect of accounting for soil flexibility, a coupled vehicle/track simulation is conducted. In this case, a half-bogie model is employed, treating the wheelset, bogie frame, and car body as rigid bodies with masses $m_c = 13.4\,\text{t}$, $m_b = 1.6\,\text{t}$ and $m_w = 2\,\text{t}$ respectively as shown in Figure 10). The primary and secondary suspensions are modelled using linear springs k_i and dampers d_i ($i = 1$ or 2), with values $k_1 = 0.61\,\text{MN/m}$, $k_2 = 1.05\,\text{MN/m}$, $d_1 = 20\,\text{kNs/m}$ and $d_2 = 5\,\text{kNs/m}$. The wheel-rail interaction is governed by the force $F_{\text{rail/wheel}}$, following Hertz's contact law. The track configuration corresponds to the high-speed line in Mévergnies, Belgium [18].

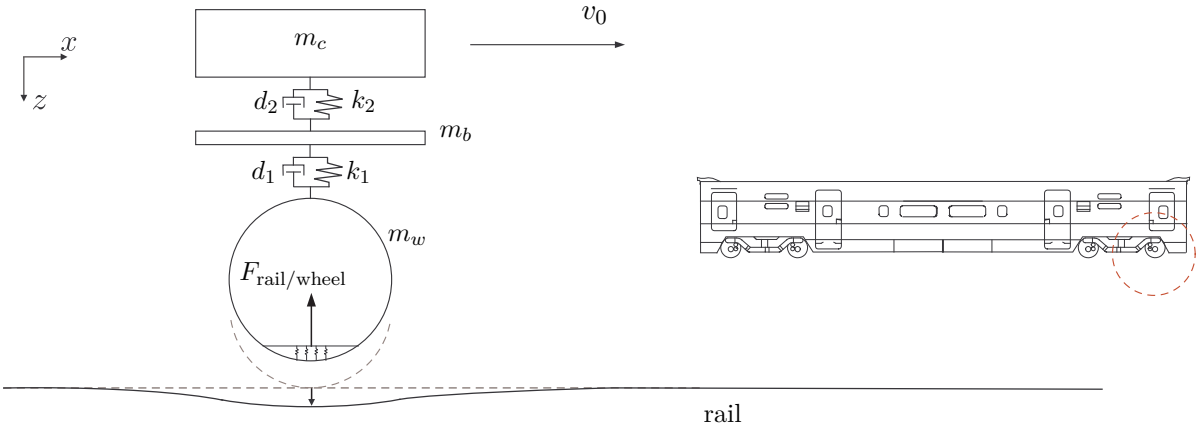

FIGURE 10 – Single–axle load vehicle model

The results obtained from the vehicle/track/foundation model, incorporating the CLM model for the foundation, are compared with those derived from a simplified Lysmer analogue model, considering two cases : stiff soil $k_b/k_f = 0.3$ and soft soil $k_b/k_f = 1.6$ (Figures 11 and 12). Differences can be observed between the two ways of considering the soil, but they are significant enough to highlight the coupling effect between sleepers through the soil. This difference becomes even more pronounced as the soil becomes more flexible relative to the track.

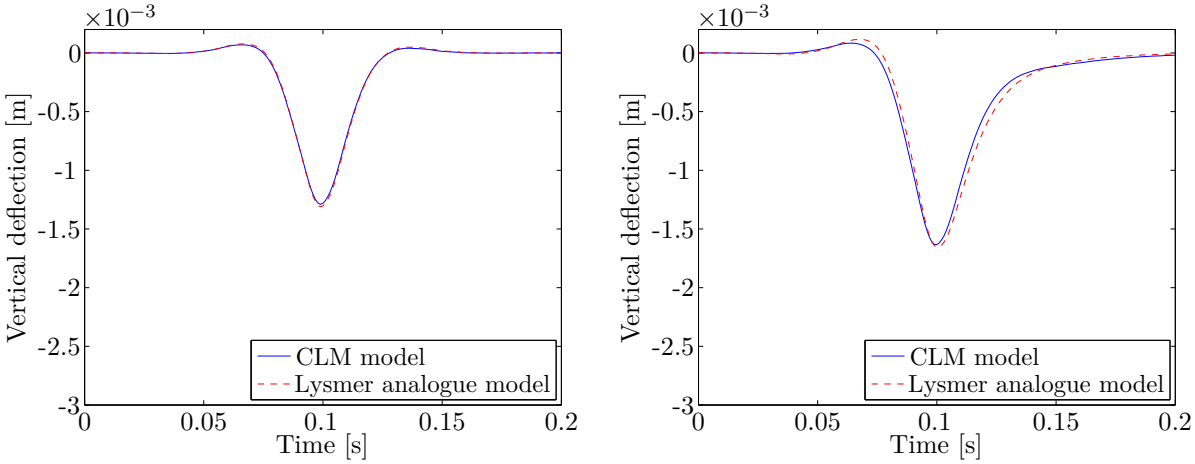

(a) Stiff soil (b) Soft soil

FIGURE 11 – Time history of the vertical rail deflection during the passing of a single–axle load vehicle at speed $v_0 = 300\,\mathrm{km/h}$

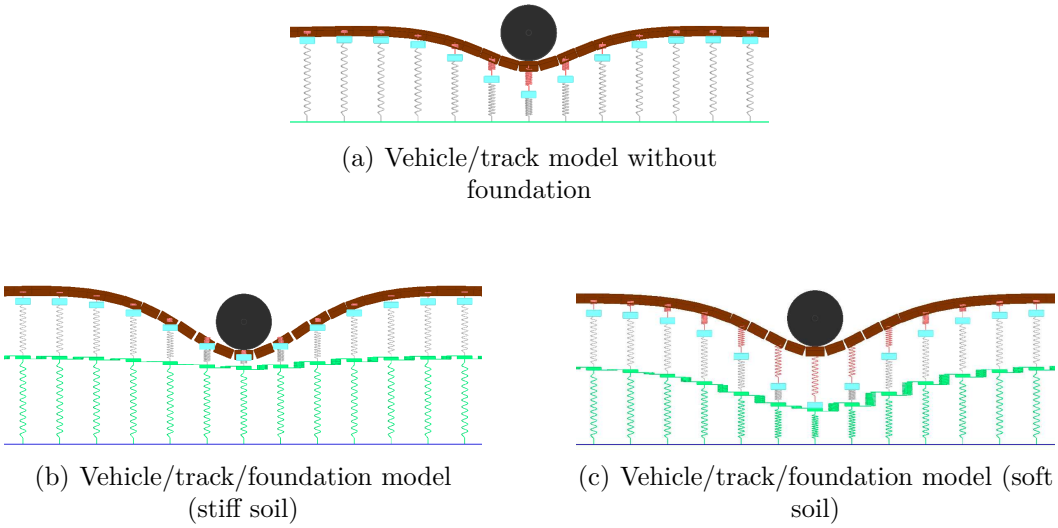

(a) Vehicle/track model without foundation

(b) Vehicle/track/foundation model (stiff soil)

(c) Vehicle/track/foundation model (soft soil)

FIGURE 12 – Visualisation of the track/foundation model during the passage of a single-axle load vehicle at a speed of $v_0 = 300\,\mathrm{km/h}$ (deformation scale factor : 500 for the rail, 1000 for the subgrade)

5 Conclusion

To simplify vehicle/track/soil simulations and avoid the complexity of a compound model, a discrete and lightweight soil representation, known as the CLM model, has been developed. This model incorporates coupling through the track contact area and is based on Lysmer analogue foundation. Interaction between foundations is captured using coupling spring and damper elements. To calibrate the dynamic parameters of the model, concise expressions for overall impedances have been formulated to match the discrete model parameters. These expressions facilitate efficient comparisons between discrete and numerical models. A fitting process, sup-

ported by a neural network, is introduced using these simplified analytical relations, similar to those in Lysmer's analogue model. The CLM model exhibits strong agreement with numerical results from finite/infinite element soil modeling across different scenarios, including homogeneous soil and layered media. Ultimately, closed-form solutions are derived, offering a fast and practical method for estimating CLM model parameters for typical soil configurations.

Références

[1] D. P. Connolly, G. Kouroussis, O. Laghrouche, C. Ho, and M. C. Forde. Benchmarking railway vibrations — track, vehicle, ground and building effects. *Construction and Building Materials*, 92 :64–81, 2015.

[2] D. J. Thompson, G. Kouroussis, and E. Ntotsios. Modelling, simulation and evaluation of ground vibration caused by rail vehicles. *Vehicle System Dynamics*, 57(7) :936–983, 2019.

[3] G. Kouroussis, D. P. Connolly, and O. Verlinden. Railway induced ground vibrations — a review of vehicle effects. *International Journal of Rail Transportation*, 2(2) :69–110, 2014.

[4] S. Dietz, G. Hippmann, and G. Schupp. Interaction of vehicles and flexible tracks by co-simulation of multibody vehicle systems and finite element track models. *Vehicle System Dynamics Supplement (The Dynamics of Vehicles on Roads and on Tracks)*, 37 :372–384, 2002.

[5] P. Galvín, A. Romero, and J. Domínguez. Fully three-dimensional analysis of high-speed train–track–soil–structure dynamic interaction. *Journal of Sound and Vibration*, 329(24) :5147–5163, 2010.

[6] K. Knothe and Y. Wu. Receptance behaviour of railway track and subgrade. *Archive of Applied Mechanics*, 68 :457–470, 1998.

[7] B. Olivier, O. Verlinden, and G. Kouroussis. A vehicle/track/soil model using co-simulation between multibody dynamics and finite element analysis. *International Journal of Rail Transportation*, 8(2) :135–158, 2020.

[8] B. Olivier, O. Verlinden, and G. Kouroussis. Comparison of X–T and X–X co-simulation techniques applied on railway dynamics. *Multibody System Dynamics*, 55(1-2) :39–56, 2022.

[9] W. Sarfeld, S. A. Savidis, R. Schuppe, and H. Klapperich. Three–dimensional dynamic interaction of ties. In *Xth ICSMFE (Internationale Baugrundtagung)*, volume 3, pages 287–292, Stockholm (Sweden), 1981.

[10] W. Rücker and L. Auersch. A user-friendly prediction tool for railway induced ground vibrations : Emission – transmission – immission. In Springer / Heidelberg, editor, *Noise and Vibration Mitigation for Rail Transportation Systems : Proceedings of the 9th International Workshop on Railway Noise* , volume 99, pages 129–135, Berlin (Germany), 2008. SpringerLink.

[11] G. Kouroussis and O. Verlinden. Prediction of railway ground vibrations : accuracy of a coupled lumped mass model for representing the track/soil interaction. *Soil Dynamics and Earthquake Engineering*, 69 :220–226, 2015.

[12] G. Kouroussis, G. Gazetas, I. Anastasopoulos, C. Conti, and O. Verlinden. Discrete modelling of vertical track–soil coupling for vehicle–track dynamics. *Soil Dynamics and Earthquake Engineering*, 31(12) :1711–1723, 2011.

[13] G. Kouroussis, O. Verlinden, and C. Conti. A two–step time simulation of ground vibrations induced by the railway traffic. *Journal of Mechanical Engineering Science*, 226(2) :454–472, 2012.

[14] G. Kouroussis, J. Florentin, and O. Verlinden. Ground vibrations induced by intercity/interregion trains : A numerical prediction based on the multibody/finite element modeling approach. *Journal of Vibration and Control*, 22(20) :4192–4210, 2016.

[15] G. Kouroussis. *Predicting high-speed railway vibration using time-domain numerical engineering approaches*, pages 187–216. ICE Publishing, 2019.

[16] G. Gazetas. Analysis of machine foundation vibrations : state of the art. *Soil Dynamics and Earthquake Engineering*, 2(1) :2–42, 1983.

[17] Charu C. Aggarwal. *Neural Networks and Deep Learning*. Springer Cham, 2023.

[18] G. Kouroussis, O. Verlinden, and C. Conti. Free field vibrations caused by high-speed lines : measurement and time domain simulation. *Soil Dynamics and Earthquake Engineering*, 31(4) :692–707, 2011.